Securing the UAV-Aided Non-Orthogonal Downlink in the Face of Colluding Eavesdroppers

Huabo Fu, Zhichao Sheng, Ali A. Nasir, Ali H. Muqaibel, and Lajos Hanzo

Abstract—Non-orthogonal unmanned aerial vehicle (UAV)-aided secure downlink transmissions are investigated. A single-antenna UAV serves multiple ground users in the face of multiple colluding eavesdroppers (EVs) and only imperfect location information of the EVs is available. Specially, a power splitting based secure non-orthogonal downlink transmission scheme is considered, where the transmit power is divided into two parts for transmitting confidential information and artificial noise. Explicitly, we maximize the minimum average secrecy rate among all the users by optimizing the UAV trajectory, the transmit power and the power splitting ratio. In order to tackle this non-convex optimization problem, we propose an iterative algorithm based on the block coordinate descent and successive convex approximation techniques. Numerical results demonstrate the superiority of our proposed algorithm.

Index Terms—Unmanned aerial vehicle, non-orthogonal transmission, secure transmission, colluding eavesdroppers, artificial noise.

I. INTRODUCTION

As a promising B5G/6G technique, unmanned aerial vehicle (UAV)-aided communication has received considerable attention as a benefit of its flexible deployment. Since a UAV hovers over the ground, it tends to have higher probability of line-of-sight (LoS) links than terrestrial communication [1], [2]. However, due to the broadcast nature of wireless channels, the availability of a LoS link makes air-to-ground communication more susceptible to eavesdropping. This emphasizes the importance of improving the security in UAV-enabled communication.

On the other hand, non-orthogonal transmission (NOTx) has the potential of significantly increasing the spectral efficiency and user fairness [3]. While conventional orthogonal transmission (OTx) relies on orthogonal time- or frequency-blocks for accommodating multiple users, the NOTx principle allows us to exploit the resources more efficiently. As a result, the NOTx philosophy has been widely applied to UAV-aided communication [4]–[6]. Given the importance of securing UAV-aided communication, several researchers have studied its security aspects as well [7]–[14]. However, these studies tend to focus on power allocation and UAV trajectory design to avoid eavesdroppers (EVs), which limits the secrecy rate

Huabo Fu and Zhichao Sheng are with Shanghai Institute for Advanced Communication and Data Science, Key Laboratory of Specialty Fiber Optics and Optical Access Networks, Shanghai University, Shanghai 200444, China (email: huabfff@shu.edu.cn; zcsheng@shu.edu.cn).

Ali A. Nasir and Ali H. Muqaibel are with the Department of Electrical Engineering and Center for Communication Systems and Sensing at King Fahd University of Petroleum and Minerals (KFUPM), Dhahran 31261, Saudi Arabia (e-mail: anasir@kfupm.edu.sa; muqaibel@kfupm.edu.sa).

Lajos Hanzo is with the School of ECS, University of Southampton, SO17 1BJ, UK (email:lh@ecs.soton.ac.uk)

attained in the presence of multiple colluding EVs or if the EVs move closer to the legitimate users for improving their eavesdropping channel. We explicitly contrast the novelty of our paper to the related literature in Table I.

Against the above background, we investigate the security of the UAV-aided non-orthogonal downlink transmissions in the presence of multiple colluding EVs, for whom we only have imperfect location information. To enhance the security, we adopt a power splitting (PS) based secure transmission scheme, where a certain portion of the transmit power is used for legitimate communication, while the remaining portion is used to transmit a jamming signal. Our goal is to maximize the minimum secrecy rate among all ground users by jointly optimizing the UAV trajectory, the transmit power, and the power splitting ratio, which is a computationally intractable non-convex problem. We apply an iterative algorithm based on the block coordinate descent (BCD) and successive convex approximation (SCA) approaches. Numerical results show the superiority of our proposed algorithm compared to the existing solutions in the literature.

II. SYSTEM MODEL AND PROBLEM FORMULATION

As is depicted in Fig.1, a single-antenna UAV serves K user equipment (UEs) on the ground, each equipped with a single antenna, under a strong eavesdropping channel. Specifically, the eavesdropping channel is termed strong, because there are M colluding EVs, whose location is only imperfectly known and they are located in close proximity of the UEs. In this extreme scenario, conventional power allocation and trajectory design alone fails to guard against EVs.

Nonetheless, to facilitate the trajectory design, we divide the scheduled flight duration T into N equal time-slots (TSs) having a duration δ, so that $T = N\delta$. The horizontal position of UE k is set to $\mathbf{Q}_k^B = \{x_k^B, y_k^B\}$, but the positions of EVs are uncertain. Hence the actual horizontal position of EV m is $\mathbf{Q}_m^E = \{x_m^E + \triangle x_m, y_m^E + \triangle y_m\}$, where $\{x_m^E, y_m^E\}$ and $\|\{\triangle x_m, \triangle y_m\}\| \le r_m$ denote the estimated horizontal position and the uncertainty range of EV m, respectively. The time-varying horizontal position of the UAV is denoted by $\mathbf{Q}_n \triangleq \{x_n, y_n\}$ with $1 \le n \le N$ and its mobility constraints can be written as

$$\|\mathbf{Q}_n - \mathbf{Q}_{n-1}\| \le v_{\max}\delta, \ n = 1, 2, 3, \ldots, N \quad (1)$$

$$\|\mathbf{Q}_F - \mathbf{Q}_N\| \le v_{\max}\delta, \quad (2)$$

where $\mathbf{Q}_0$ and $\mathbf{Q}_F$ denote the initial position and final position of the UAV, respectively, while $v_{\max}$ is the maximum horizontal speed of the UAV.

Again, the air-to-ground (A2G) channels are dominated by LoS propagation, especially in rural and sub-urban scenarios

TABLE I: OUR NOVEL CONTRIBUTIONS CONTRASTED TO THE STATE-OF-THE-ART

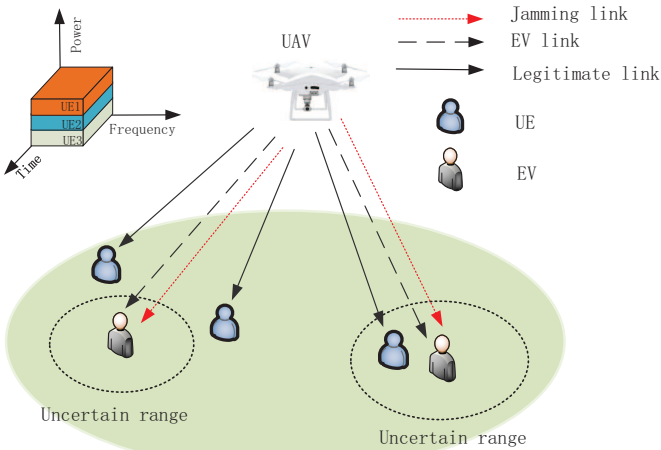|	Our paper	[7]	[8]	[9], [10]	[11]	[12]	[13]	[14]
Imperfect Location Information of EVs	✓	✓						✓
Colluding EVs	✓					✓		✓
Trajectory Optimization	✓		✓		✓	✓	✓	✓
Power Allocation	✓	✓	✓	✓	✓	✓	✓	
Power-Splitting based Artificial Noise	✓						✓	
Non-orthogonal Transmission	✓			✓	✓			
UE is within uncertain range of EV	✓							

Fig. 1: System model.

[2], [15], as shown by the 3GPP field trials. For analytical convenience, we assume that the A2G channels follow the free space model, i.e., the channel gain from the UAV to UE k over TS n is $h^U_{k,n}(\mathbf{Q}) = \frac{\beta_0}{\|\mathbf{Q}_n - \mathbf{Q}^B_k\|^2 + H^2}$, and that from the UAV to EV m over TS n is $h^E_{n,m}(\mathbf{Q}) = \max_{\{\triangle x_m, \triangle y_m\}} \frac{\beta_0}{\|\mathbf{Q}_n - \mathbf{Q}^E_m\|^2 + H^2}$, where β_0 denotes the channel power gain at the reference distance and H is the altitude of the UAV.

To counteract the colluding EVs, a popular technique is to insert artificial noise (AN) into the null-space of legitimate receivers [16]. However, that is only possible for multiple antennas. Therefore, in our single-antenna scenario, we adopt power splitting based transmission, where the transmit power $P_{k,n}$ of TS n is divided into two parts using a power splitting ratio of $0 \leq \alpha_n \leq 1$. Explicitly, the UAV transmits a jamming signal of $(1-\alpha_n)P_{k,n}$, while it performs legitimate transmission of $\alpha_n P_{k,n}$, where the specifically designed AN can be eliminated by legitimate receivers, but not necessarily by the EVs [17]. The transmit power constraint can be expressed as

$$\sum_{k=1}^{K} P_{k,n} \leq P_{\max}, \ \forall n, \quad (3)$$

where $P_{\max}$ denotes the maximum transmit power budget of the UAV. Let us define $P^U_{k,n} \triangleq \alpha_n P_{k,n}$ and $P^E_{k,n} \triangleq (1-\alpha_n)P_{k,n}$. Hence the constraint (3) is rewritten as

$$\sum_{k=1}^{K} (P^E_{k,n} + P^U_{k,n}) \leq P_{\max}, \ \forall n. \quad (4)$$

In our downlink NOTx scheme, each UE employs the popular successive interference cancellation (SIC) technique, which is based on the UAV-UE channel gain. Specifically, assume that the channel gains of the UAV-UE links are sorted in descending order w.r.t their time-varying index $f_n(j)$, which is a one-to-one mapping:

$$h^U_{f_n(1),n}(\mathbf{Q}) \geq h^U_{f_n(2),n}(\mathbf{Q}) \geq ... \geq h^U_{f_n(K),n}(\mathbf{Q}), \quad (5)$$

where j denotes the index sorted in ascending order, while $f_n(j)$ denotes the resorted index j over TS n. The transmit power is allocated in the reverse order of (5)

$$P^U_{f_n(1),n} \leq P^U_{f_n(2),n} \leq \cdots \leq P^U_{f_n(K),n}. \quad (6)$$

Let $\mathbf{P} \triangleq \{P^E_{k,n} \geq 0, P^U_{k,n} \geq 0, \forall n, k\}$ denote the set of transmit powers and σ^2 represent the power of additive white Gaussian noise (AWGN) at the receivers. Then the information throughput of UE k in bits/sec/Hz (bps/Hz) over TS n is given by

$$r^U_{k,n}(\mathbf{Q}, \mathbf{P}) = \log_2 \left[1 + \rho^U_{k,n}(\mathbf{Q}, \mathbf{P})\right], \quad (7)$$

where $\rho^U_{k,n}(\mathbf{Q}, \mathbf{P}) \triangleq \frac{h^U_{k,n} P^U_{k,n}}{\sigma^2 + h^U_{k,n} \sum_{i \in \mathbf{\Omega}_{k,n}} P^U_{i,n}}$ is the signal-to-noise ratio (SNR) of UE k over TS n. The set $\mathbf{\Omega}_{k,n}$ is defined as follows:

$$\mathbf{\Omega}_{k,n} = \begin{cases} \{f_n(i), \ 1 \leq i < f_n^{-1}(k)\}, & \text{for } f_n^{-1}(k) > 1 \\ \varnothing, & \text{for } f_n^{-1}(k) = 1 \end{cases}$$

where $f_n^{-1}(k)$ is the inverse function of the mapping $f_n(j)$. The throughput of the colluding EVs in bps/Hz over TS n is given by [14]:

$$r^E_{k,n}(\mathbf{Q}, \mathbf{P}) = \log_2 \left(1 + \sum_{m=1}^{M} \rho^E_{k,n,m}(\mathbf{Q}, \mathbf{P})\right), \quad (8)$$

where

$$\rho^E_{k,n,m}(\mathbf{Q}, \mathbf{P}) \triangleq \frac{h^E_{n,m} P^U_{k,n}}{\sigma^2 + h^E_{n,m} \left(\sum_{i \neq k}^{K} P^U_{i,n} + \sum_{i=1}^{K} P^E_{i,n}\right)} \quad (9)$$

is the SNR of EV m overhearing the transmission of UE k in TS n.

Now our objective is to maximize the minimum secrecy downlink throughput among all legitimate links by optimizing the power allocation $\mathbf{P}$ and UAV trajectory $\mathbf{Q} = \{\mathbf{Q}_n, \forall n\}$. The power splitting ratio $\boldsymbol{\alpha} = \{\alpha_n, \forall n\}$ will be derived later using $\mathbf{P}$. Upon defining the secure rate as $r^S_{k,n}(\mathbf{Q}, \mathbf{P}) \triangleq$

$[r_{k,n}^U(\mathbf{Q},\mathbf{P}) - r_{k,n}^E(\mathbf{Q},\mathbf{P})]^+$, where $[x]^+ \triangleq \max(x,0)$, the optimization problem is formulated as:

$$\max_{\mathbf{Q},\mathbf{P}} \min_k \quad \frac{1}{N}\sum_n r_{k,n}^S(\mathbf{Q},\mathbf{P}) \tag{10a}$$

$$\text{s.t.} \quad (1),(2),(4),(6). \tag{10b}$$

The optimization problem (10) is difficult to solve due to the following reasons. Firstly, the objective function (OF) (10a) is non-smooth because of the operator $[\cdot]^+$. Secondly, the problem (10) is still non-convex due to the coupled variables $\{\mathbf{Q},\mathbf{P}\}$ even without $[\cdot]^+$. Lastly, the time varying decoding order in the downlink NOTx scheme makes the problem (10) complex. Thus, the problem (10) is a standard NP-hard problem, hence it is computationally intractable.

III. THE PROPOSED ALGORITHM

To this end, according to Lemma 1 in [18], we can handle the non-smooth nature of the OF (10a), thus problem (10) has the same optimal solution as the following problem:

$$\max_{\mathbf{Q},\mathbf{P}} \min_k \quad \frac{1}{N}\sum_n [r_{k,n}^U(\mathbf{Q},\mathbf{P}) - r_{k,n}^E(\mathbf{Q},\mathbf{P})] \tag{11a}$$

$$\text{s.t.} \quad (1),(2),(4),(6). \tag{11b}$$

By introducing a slack variable λ, (11) can be rewritten as

$$\max_{\mathbf{Q},\mathbf{P},\lambda} \quad \lambda \tag{12a}$$

$$\text{s.t.} \quad (1),(2),(4),(6) \tag{12b}$$

$$\frac{1}{N}\sum_n [r_{k,n}^U(\mathbf{Q},\mathbf{P}) - r_{k,n}^E(\mathbf{Q},\mathbf{P})] \geq \lambda, \ \forall k. \tag{12c}$$

The problem (11) is equivalent to problem (12), because λ is the lower bound on the secrecy rate $\frac{1}{N}\sum_n [r_{k,n}^U(\mathbf{Q},\mathbf{P}) - r_{k,n}^E(\mathbf{Q},\mathbf{P})]$ for any k.

Then we decompose (12) into two subproblems by applying the BCD method [18], [19]. One of the subproblems is to optimize the UAV trajectory at a fixed power, while the other is to perform optimal power allocation. We also update the SIC detection order after optimizing the trajectory.

A. Trajectory optimization

Firstly, given a fixed power allocation $\mathbf{P}^{(\kappa)}$, the optimization subproblem is formulated as

$$\max_{\mathbf{Q},\lambda} \quad \lambda \qquad \text{s.t.} \quad (1),(2),(12c), \tag{13}$$

where the problem is non-convex, which is mainly caused by the non-concave left hand side (LHS) of (12c). To invoke convex approximation, we firstly rewrite the LHS of (12c) as follows:

$$r_{k,n}^S(\mathbf{Q}) \triangleq \log_2\left(1 + \frac{P_{k,n}^U}{g_{k,n}^U + \sum_{i\in\mathbf{\Omega}_{k,n}} P_{i,n}^U}\right)$$
$$- \log_2\left(1 + \sum_{m=1}^M \frac{P_{k,n}^U}{g_{n,m}^E + \sum_{i\neq k} P_{i,n}^U + \sum_{i=1}^K P_{i,n}^E}\right), \tag{14}$$

where $g_{k,n}^U \triangleq \frac{\|\mathbf{Q}_n - \mathbf{Q}_k^U\|^2 + H^2}{\gamma}$, $g_{n,m}^E \triangleq \frac{1}{\gamma}\min_{\{\triangle x_m, \triangle y_m\}}\|\mathbf{Q}_n - \mathbf{Q}_m^E\|^2 + H^2$, and $\gamma \triangleq \frac{\beta_0}{\sigma^2}$. Next, we define the auxiliary variables:

$$\phi_{k,n}(\mathbf{Q}) \triangleq \frac{g_{k,n}^U + \sum_{i\in\mathbf{\Omega}_{k,n}} P_{i,n}^U}{P_{k,n}^U}$$

$$\theta_{k,n,m}(\mathbf{Q}) \triangleq g_{n,m}^E + \sum_{i\neq k} P_{i,n}^U + \sum_{i=1}^K P_{i,n}^E. \tag{15}$$

To handle the infinite number of points in $\{\triangle x_m, \triangle y_m\}$, we consider the popular S-procedure of [20] for the double inequality alternative problem. Firstly, we introduce a slack variable $\mathbf{D} = \{D_{n,m}, \forall n, m\}$ to derive a lower bound of $\theta_{k,n,m}(\mathbf{Q})$ as

$$\theta_{k,n,m}(\mathbf{Q}) \geq \frac{1}{\gamma}D_{n,m} + \sum_{i\neq k} P_{i,n}^U + \sum_{i=1}^K P_{i,n}^E$$
$$\triangleq \theta_{k,n,m}^{\text{low}}(\mathbf{D}), \tag{16}$$

where we have:

$$D_{n,m} - \min_{\{\triangle x_m, \triangle y_m\}}\|\mathbf{Q}_n - \mathbf{Q}_m^E\|^2 - H^2 \leq 0, \tag{17a}$$

$$\|\{\triangle x_m, \triangle y_m\}\|^2 - r_m^2 \leq 0. \tag{17b}$$

According to the S-procedure, the necessity and sufficiency of (17a) determined by (17b) is that there exists a point set $\epsilon = \{\epsilon_{n,m} \geq 0, \forall n, m\}$ so that $\mathbf{\Psi}(\mathbf{Q}_n, D_{n,m}, \epsilon_{n,m}) \succeq \mathbf{0}$, where we have:

$$\mathbf{\Psi}(\mathbf{Q}_n, D_{n,m}, \epsilon_{n,m})$$
$$= \begin{bmatrix} (\epsilon_{n,m}+1)\mathbf{I}_2 & \mathbf{Q}_m^E - \mathbf{Q}_n \\ [\mathbf{Q}_m^E - \mathbf{Q}_n]^H & -(r_m)^2\epsilon_{n,m} + C_{n,m} \end{bmatrix} \succeq \mathbf{0} \tag{18}$$

and

$$C_{n,m} = \|\mathbf{Q}_n - \mathbf{Q}_m^E\|^2 + H^2 - D_{n,m}. \tag{19}$$

Introducing a slack variable $\boldsymbol{\vartheta} = \{\vartheta_{k,n}, \forall k, n\}$, the lower bound of (14) is given by

$$r_{k,n}^{S,\text{low}}(\mathbf{Q},\boldsymbol{\vartheta}) \triangleq \log_2\left(1 + \frac{1}{\phi_{k,n}(\mathbf{Q})}\right) - \log_2(1 + \vartheta_{k,n}), \tag{20}$$

which is constrained by

$$\sum_{m=1}^M \frac{P_{k,n}^U}{\theta_{k,n,m}^{\text{low}}(\mathbf{D})} \leq \vartheta_{k,n}, \ \forall k, n. \tag{21}$$

Upon using (20)-(21), the problem (13) can be written as:

$$\max_{\mathbf{Q},\boldsymbol{\vartheta},\mathbf{D},\lambda} \quad \lambda \tag{22a}$$

$$\text{s.t.} \quad (1),(2),(18),(21) \tag{22b}$$

$$\epsilon_{n,m} \geq 0, \quad \forall n, m \tag{22c}$$

$$\frac{1}{N}\sum_n r_{k,n}^{S,\text{low}}(\mathbf{Q},\boldsymbol{\vartheta}) \geq \lambda, \ \forall k. \tag{22d}$$

Note that the constraints (18) and (22d) are nonconvex, making (22) a computationally challenging nonconvex problem. To handle the constraints (18) and (22d), we have to derive their inner approximations. Let $(\mathbf{Q}^{(\kappa)}, \mathbf{D}^{(\kappa)}, \boldsymbol{\vartheta}^{(\kappa)})$ be

a feasible point for (22) that is found from the $(\kappa - 1)$-st iteration. In order to generate the next feasible point $(\mathbf{Q}^{(\kappa+1)}, \mathbf{D}^{(\kappa+1)}, \boldsymbol{\vartheta}^{(\kappa+1)})$ for (22), we first have to approximate (19) by a lower bound at the κ-th iteration, which is given by

$$C_{n,m}^{(\kappa)} = \|\mathbf{Q}_n^{(\kappa)} - \mathbf{Q}_m^E\|^2 + H^2 - D_{n,m} + 2(\mathbf{Q}_n^{(\kappa)} - \mathbf{Q}_m^E)^H(\mathbf{Q}_n - \mathbf{Q}_n^{(\kappa)}) \tag{23}$$

where $C_{n,m} \geq C_{n,m}^{(\kappa)}$. Therefore, the nonlinear matrix inequality in (18) is approximated by the following inequality:

$$\boldsymbol{\Psi}^{(\kappa)}\left(\mathbf{Q}_n, D_{n,m}, \epsilon_{n,m}\right)$$
$$= \begin{bmatrix} (\epsilon_{n,m} + 1)\mathbf{I}_2 & \mathbf{Q}_m^E - \mathbf{Q}_n \\ [\mathbf{Q}_m^E - \mathbf{Q}_n]^H & -(r_m)^2\epsilon_{n,m} + C_{n,m}^{(\kappa)} \end{bmatrix} \succeq \mathbf{0}. \tag{24}$$

Next, we derive a lower bounding concave approximation of (20) by exploiting the convexity of $\log(1 + 1/x)$ and the concavity of $\log(1 + x)$, yielding:

$$r_{k,n}^{S,\text{low}}(\mathbf{Q}, \boldsymbol{\vartheta}) \geq a_{k,n}^{(\kappa)} + b_{k,n}^{(\kappa)} + c_{k,n}^{(\kappa)}(\phi_{k,n}(\mathbf{Q}) - \phi_{k,n}(\mathbf{Q}^{(\kappa)}))$$
$$+ d_{k,n}^{(\kappa)}(\vartheta_{k,n} - \vartheta_{k,n}^{(\kappa)})$$
$$\triangleq r_{k,n}^{S,(\kappa)}(\mathbf{Q}, \boldsymbol{\vartheta}), \tag{25}$$

where $a_{k,n}^{(\kappa)} = \log_2\left(1 + \frac{1}{\phi_{k,n}(\mathbf{Q}^{(\kappa)})}\right)$, $b_{k,n}^{(\kappa)} = \log_2(1 + \vartheta_{k,n}^{(\kappa)})$, $c_{k,n}^{(\kappa)} = -\frac{1}{\ln 2(\phi_{k,n}(\mathbf{Q}^{(\kappa)}) + (\phi_{k,n}(\mathbf{Q}^{(\kappa)}))^2)}$, and $d_{k,n}^{(\kappa)} = \frac{1}{\ln 2(1 + \vartheta_{k,n}^{(\kappa)})}$. Therefore, at the κ-th iteration, the following convex problem is solved for generating the next feasible point $(\mathbf{Q}^{(\kappa+1)}, \mathbf{D}^{(\kappa+1)}, \boldsymbol{\vartheta}^{(\kappa+1)})$ for (22):

$$\max_{\mathbf{Q}, \boldsymbol{\vartheta}, \mathbf{D}, \lambda} \quad \lambda \tag{26a}$$
$$\text{s.t.} \quad (1), (2), (21), (22c), (24), \tag{26b}$$
$$\frac{1}{N}\sum_n r_{k,n}^{S,(\kappa)}(\mathbf{Q}, \boldsymbol{\vartheta}) \geq \lambda, \quad \forall k. \tag{26c}$$

B. Power allocation

In this subsection, we focus our attention on the power allocation problem for a fixed trajectory and decoding order. The subproblem is formulated as follows:

$$\max_{\mathbf{P}, \lambda} \quad \lambda \tag{27a}$$
$$\text{s.t.} \quad (4), (6), (12c), \tag{27b}$$

where the LHS of (12c) is non-concave, making the problem non-convex. By introducing auxiliary variables, we have:

$$\pi_{k,n}(\mathbf{P}) \triangleq g_{k,n}^U + \sum_{i \in \boldsymbol{\Omega_k}} P_{i,n}^U$$

$$\varpi_{k,n}(\mathbf{P}) \triangleq \frac{1}{P_{k,n}^U}$$

$$\nu_{k,n,m}(\mathbf{P}) \triangleq g_{n,m}^E + \sum_{i \neq k} P_{i,n}^U + \sum_{i=1}^K P_{i,n}^E,$$

and $\boldsymbol{\omega} = \{\omega_{k,n}, \forall k, n\}$. Then, a lower bound of the LHS of (12c) is given by

$$r_{k,n}^S(\mathbf{P}) \geq \log_2\left(1 + \frac{1}{\pi_{k,n}(\mathbf{P})\varpi_{k,n}(\mathbf{P})}\right) - \log_2(1 + \omega_{k,n})$$
$$\triangleq r_{k,n}^{S,\text{low}}(\mathbf{P}, \boldsymbol{\omega}), \tag{28}$$

under the following constraint:

$$\sum_{m=1}^U \frac{P_{k,n}^U}{\nu_{k,n,m}(\mathbf{P})} \leq \omega_{k,n}, \quad \forall k, n. \tag{29}$$

Since (29) is a non-convex constraint, we again develop an iterative procedure to first approximate (29) by the following convex constraint at the κ-th iteration [21, (76)]:

$$\sum_{m=1}^M \frac{(P_{k,n}^U)^2/P_{k,n}^{U,(\kappa)} + P_{k,n}^{U,(\kappa)}}{2\nu_{k,n,m}(\mathbf{P})} \leq \omega_{k,n}, \quad \forall k, n, \tag{30}$$

Next, we derive a lower bounding concave approximation of (28) by exploiting the convexity of $\log(1 + 1/xy)$, i.e.,

$$r_{k,n}^{S,\text{low}}(\mathbf{P}, \boldsymbol{\omega}) \geq \ell_{k,n}^{(\kappa)} + \varsigma_{k,n}^{(\kappa)} + \imath_{k,n}^{(\kappa)}\left(2 - \frac{\pi_{k,n}(\mathbf{P})}{\pi_{k,n}(\mathbf{P}^{(\kappa)})}\right.$$
$$\left. - \frac{\varpi_{k,n}(\mathbf{P})}{\varpi_{k,n}(\mathbf{P}^{(\kappa)})}\right) + \xi_{k,n}^{(\kappa)}(\omega_{k,n} - \omega_{k,n}^{(\kappa)})$$
$$\triangleq r_{k,n}^{S,(\kappa)}(\mathbf{P}), \tag{31}$$

where $\ell_{k,n}^{(\kappa)} = \log_2(1 + \frac{1}{\pi_{k,n}(\mathbf{P}^{(\kappa)})\varpi_{k,n}(\mathbf{P}^{(\kappa)})})$, $\varsigma_{k,n}^{(\kappa)} = \log_2(1 + \omega_{k,n}^{(\kappa)})$, $\imath_{k,n}^{(\kappa)} = \frac{1}{(1 + \pi_{k,n}(\mathbf{P}^{(\kappa)})\varpi_{k,n}(\mathbf{P}^{(\kappa)}))\ln 2}$, and $\xi_{k,n}^{(\kappa)} = \frac{1}{(1 + \omega_{k,n}^{(\kappa)})\ln 2}$. Therefore, at the κ-th iteration, we solve the following convex problem:

$$\max_{\mathbf{P}, \lambda} \quad \lambda \tag{32a}$$
$$\text{s.t.} \quad (4), (6), (30) \tag{}$$
$$\frac{1}{N}\sum_n r_{k,n}^{S,(\kappa)}(\mathbf{P}) \geq \lambda, \quad \forall k. \tag{32b}$$

C. Overall Algorithm

The non-convex problem (10) can be solved by iteratively solving (26) and (32) as well as adjusting the decoding order. The power splitting ratio $\boldsymbol{\alpha}$ and the total transmit power $\{P_{k,n}, \forall k, n\}$ can be reconstructed according to $\alpha_n = \sum_{k=1}^K \frac{P_{k,n}^U}{P_{k,n}^E + P_{k,n}^U}$ and $P_{k,n} = P_{k,n}^E + P_{k,n}^U$, respectively. To ensure optimal power allocation as possible, we propose a double-loop based iterative algorithm, as outlined in Alg. 1. Specifically in the inner loop, the transmit power is iteratively optimized to compensate for the loss of the OF owing to adjusting the decoding order.

D. Complexity and Convergence Analysis

Let us define $\lambda(\mathbf{P}, \mathbf{Q})$, $\lambda_{\text{trj}}^{(\kappa)}(\mathbf{P}, \mathbf{Q})$ and $\lambda_{\text{pow}}^{(\kappa)}(\mathbf{P}, \mathbf{Q})$ as the OF of problems (10), (26) and (32), respectively. Then we have

$$\lambda(\mathbf{P}^{(\kappa)}, \mathbf{Q}^{(\kappa)}) \overset{(a)}{=} \lambda_{\text{trj}}^{(\kappa)}(\mathbf{P}^{(\kappa)}, \mathbf{Q}^{(\kappa)})$$
$$\overset{(b)}{\leq} \lambda_{\text{trj}}^{(\kappa)}(\mathbf{P}^{(\kappa)}, \mathbf{Q}^{(\kappa+1)})$$
$$\overset{(c)}{\leq} \lambda(\mathbf{P}^{(\kappa)}, \mathbf{Q}^{(\kappa+1)}), \tag{33}$$

where (a) holds true since the Taylor expansions in (24) and (25) are tight at the given feasible points; (b) holds true through trajectory optimization; (c) holds true since the OF

Algorithm 1 Algorithm Proposed for Solving (10)

1: **Initialization:** Set $\kappa = 0$. Find a set of initial feasible solution $(\mathbf{Q}^{(\kappa)}, \mathbf{P}^{(\kappa)})$ for (10), and get an initial decoding order according to (5)
2: **Repeat outer loop**
3:     Solve problem (26) to generate the optimal trajectory $(\mathbf{Q}^{(\kappa+1)})$ with fixed power $(\mathbf{P}^{(\kappa)})$.
4:     Update the decoding order according to (5).
5:     **Repeat inner loop**
6:         Solve problem (32) to generate the optimal power $(\mathbf{P}^{(\kappa+1)})$ with $(\mathbf{P}^{(\kappa)})$ and fixed the trajectory $(\mathbf{Q}^{(\kappa+1)})$. Set $\mathbf{P}^{(\kappa)} := \mathbf{P}^{(\kappa+1)}$.
7:     **Until convergence of the inner loop**
8:     Set $\kappa := \kappa + 1$
9: **Until convergence of the outer loop**

---

of problem (26) is the lower bound of the OF of the original problem (10). For a given $\mathbf{Q}^{(\kappa+1)}$, it also holds true that

$$
\begin{aligned}
\lambda(\mathbf{P}^{(\kappa)}, \mathbf{Q}^{(\kappa+1)}) &= \lambda_{\text{pow}}^{(\kappa)}(\mathbf{P}^{(\kappa)}, \mathbf{Q}^{(\kappa+1)}) \\
&\leq \lambda_{\text{pow}}^{(\kappa)}(\mathbf{P}^{(\kappa+1)}, \mathbf{Q}^{(\kappa+1)}) \\
&\leq \lambda(\mathbf{P}^{(\kappa+1)}, \mathbf{Q}^{(\kappa+1)}),
\end{aligned}
\tag{34}
$$

which can be similarly explained as in (33) [22]. For a given $\mathbf{Q}^{(\kappa+1)}$, we iteratively optimize the transmit power until convergence is reached. Based on (33) and (34), it follows that

$$
\lambda(\mathbf{P}^{(\kappa)}, \mathbf{Q}^{(\kappa)}) \leq \lambda(\mathbf{P}^{(\kappa+1)}, \mathbf{Q}^{(\kappa+1)}),
\tag{35}
$$

which means that the OF value of problem (10) is non-decreasing. Therefore, Algorithm 1 converges at least to a locally optimal solution of the original nonconvex problem (10) within a polynomial complexity [18].

$$
\mathcal{O}\left(\theta' N_{out} + \theta'' N_{out} N_{in}\right),
\tag{36}
$$

where the expressions $\theta' = \sqrt{(KM + 3M + K + 2)N + 2}[X^3 + (K + 11)MNX^2]$ and $\theta'' = \sqrt{(4K + KM - 1)N}[Y^3 + (KM + 4K - 1)NY^2]$ quantify the complexity of solving the optimization problem (26) and (32), respectively. In these expressions, $X = (2M + K + 2)N + 1$ and $Y = 2KN + 1$ represent the number of variables in (26) and (32), respectively, while N_{out} and N_{in} denote the numbers of iterations in the outer loop and inner loop, respectively. Besides, the complexity of "OTx" is $O[N_{ite}(\eta' + \eta'')]$, where N_{ite} denotes the number of iterations, while $\eta' = \sqrt{(KM + 3M + 3K + 2)N + 2}[(X')^3 + (X')^2(4K + 9M)N + X'(8K + 27M)N]$, and $\eta'' = \sqrt{3KN}[(Y')^3 + KN(Y')^2 + 3KNY']$. $X' = 2N(K + M + 1) + 1$ and $Y' = KN + 1$ denote the number of the variables in the different blocks.

IV. NUMERICAL RESULTS

In this section, we quantify the proposed algorithm's performance by simulations. We set $K = 4$ ground UEs and $M = 2$ EVs. The flight duration is $T = 60$ sec and the duration of each TS is $\delta = 0.5$ sec. The UAV altitude is fixed at $H = 100$ m [23] and the maximum horizontal speed is $v_{\max} = 40$ m/s. The channel power gain at the reference distance is $\beta_0 = -50$ dB, while the noise power is set to $\sigma^2 = -110$ dBm [23]. We have used MATLAB and CVX for our simulations [24].

In our simulation results, "Proposed Alg. 1 (AN-NOTx)" refers to the proposed algorithm, while "Alg. 1 w/o traj" refers to the design of the transmit power and the power splitting ratio with fixed trajectory. For characterizing the performance of the proposed Alg. 1, we consider Scenario 1 and Scenario 2 in Figures 2 and 3, respectively. Explicitly, Scenario 2 assumes a stronger EV channel than Scenario 1, because the EVs are closer to the UEs in Scenario 2.

Under Scenario 1, Fig. 2(a) plots the UAV trajectories based on "Alg. 1 w/o traj" and "OTx". It is observed that the UAV trajectories based on the proposed Alg. 1 and OTx are similar under the weaker eavesdropping channel of Scenario 1. Fig. 2(b) plots the average secrecy rate (ASR) versus $P_{\max}$ for different algorithms. Observe that under a lower transmit power budget $P_{\max}$, "OTx" achieves better ASR than the other two algorithms. However, as the transmit power budget $P_{\max}$ increases, the ASR of "Proposed Alg. 1 (AN-NOTx)" becomes better than that of "OTx" and "Alg. 1 w/o traj". This is because the AN in the proposed Alg. 1 cannot contribute effectively in the presence of lower transmit power budgets.

Fig. 3 shows the performance attained under the stronger eavesdropping channel (Scenario 2). Fig. 3(a) plots the UAV trajectories generated by the different algorithms. Observe that under the "Proposed Alg. 1 (AN-NOTx)" scheme, the UAV safely serves all legitimate UEs, since it can send AN to confuse the EVs and secure downlink transmission to the legitimate UEs. Under "NOTx", the UAV first passes by UE-1 and UE-2, then stays away from UE-3 and flies to UE-4. This is because if UAV had flown to UE-3, its channel w.r.t. UE-1 would have become weaker than that w.r.t. EV-1, which would have made the secrecy rate of UE-1 negative. Under "OTx", the UAV stays away from all EVs and legitimate UEs, since it cannot withstand the strong eavesdropping channel. Figures 3(b) and 3(c) plots the ASR versus $P_{\max}$ and M for the different algorithms. The results show the clear and dominant supremacy of the proposed Alg. 1 over the other approaches. Note that the ASR of "OTx" is nearly zero under the strong eavesdropping channel. Finally, Fig. 3(d) shows that the proposed Alg. 1 also achieves the fastest convergence.

Fig. 4 illustrates the power splitting ratio versus time under Scenario 1 and 2. In Fig. 4(a), it can be observed that the majority of transmit power is used to perform legitimate transmission from $n = 0$ to $n = 60$. Beyond that the transmit power allocated for transmitting AN increases. In Fig. 4(b), the majority of transmit power is used to perform legitimate transmission from $n = 50$ to $n = 80$. Note that the variation in the power splitting ratio decreases upon increasing the transmit power budget.

V. CONCLUSIONS

This paper has considered secure downlink transmission from a UAV to multiple ground users in the presence of multiple colluding EVs, whose location is not known exactly. In order to guarantee secure downlink transmission, we have proposed a power splitting based secure NOTx scheme, where the transmit power is divided into two parts for transmitting confidential information and AN, respectively. The minimum
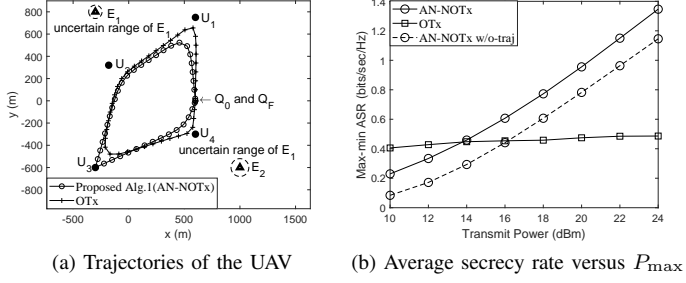
(a) Trajectories of the UAV

(b) Average secrecy rate versus $P_{\max}$

Fig. 2: Performance analysis under Scenario 1.

(a) Trajectories of the UAV

(b) Average secrecy rate versus $P_{\max}$

(c) Average secrecy rate versus M

(d) The convergence of the proposed algorithms.

Fig. 3: Performance analysis under Scenario 2
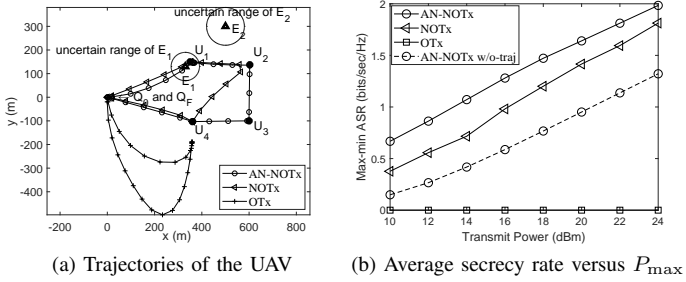

(a) Power splitting ratio under Scenario 1
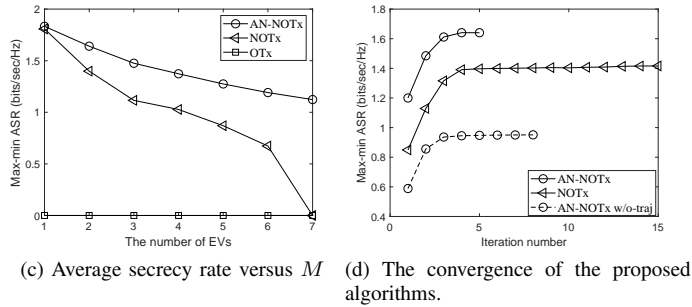
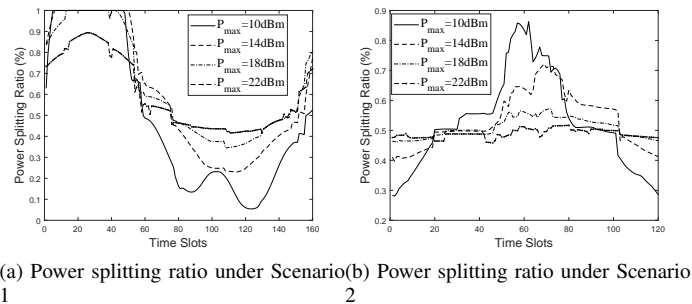(b) Power splitting ratio under Scenario 2

Fig. 4: The trend of power splitting ratio

ASR is maximized by jointly optimizing the UAV trajectory, the transmit power, and the power splitting ratio. Due to the non-convexity of the problem formulated, an iterative algorithm based on BCD and SCA approaches has been proposed. Our simulation results revealed that the proposed algorithm achieves better performance than the benchmarks.

REFERENCES

[1] Y. Zeng, R. Zhang, and T. J. Lim, "Wireless communications with unmanned aerial vehicles: opportunities and challenges," *IEEE Commun. Mag.*, vol. 54, no. 5, pp. 36–42, 2016.

[2] X. Lin, V. Yajnanarayana, S. D. Muruganathan, S. Gao, H. Asplund, H.-L. Maattanen, M. Bergstrom, S. Euler, and Y.-P. E. Wang, "The sky is not the limit: LTE for unmanned aerial vehicles," *IEEE Commun. Mag.*, vol. 56, no. 4, pp. 204–210, 2018.

[3] L. Dai, B. Wang, Y. Yuan, S. Han, I. Chih-lin, and Z. Wang, "Non-orthogonal multiple access for 5G: solutions, challenges, opportunities, and future research trends," *IEEE Commun. Mag.*, vol. 53, no. 9, pp. 74–81, 2015.

[4] A. A. Nasir, H. D. Tuan, T. Q. Duong, and H. V. Poor, "UAV-enabled communication using NOMA," *IEEE Trans. Commun.*, vol. 67, no. 7, pp. 5126–5138, 2019.

[5] N. Zhao, X. Pang, Z. Li, Y. Chen, F. Li, Z. Ding, and M.-S. Alouini, "Joint trajectory and precoding optimization for UAV-assisted NOMA networks," *IEEE Trans. Commun.*, vol. 67, no. 5, pp. 3723–3735, 2019.

[6] X. Jiang, Z. Wu, Z. Yin, Z. Yang, and N. Zhao, "Power consumption minimization of UAV relay in NOMA networks," *IEEE Wireless Commun. Lett.*, vol. 9, no. 5, pp. 666–670, 2020.

[7] T. Bai, J. Wang, Y. Ren, and L. Hanzo, "Energy-efficient computation offloading for secure UAV-edge-computing systems," *IEEE Trans. Veh. Technol.*, vol. 68, no. 6, pp. 6074–6087, 2019.

[8] G. Zhang, Q. Wu, M. Cui, and R. Zhang, "Securing UAV communications via joint trajectory and power control," *IEEE Trans. Wirel. Commun.*, vol. 18, no. 2, pp. 1376–1389, 2019.

[9] N. Zhao, Y. Li, S. Zhang, Y. Chen, W. Lu, J. Wang, and X. Wang, "Security enhancement for NOMA-UAV networks," *IEEE Trans. Veh. Technol.*, vol. 69, no. 4, pp. 3994–4005, 2020.

[10] X. Chen, Z. Yang, N. Zhao, Y. Chen, J. Wang, Z. Ding, and F. R. Yu, "Secure transmission via power allocation in NOMA-UAV networks with circular trajectory," *IEEE Trans. Veh. Technol.*, vol. 69, no. 9, pp. 10 033–10 045, 2020.

[11] H.-M. Wang and X. Zhang, "UAV secure downlink NOMA transmissions: A secure users oriented perspective," *IEEE Trans. Commun.*, vol. 68, no. 9, pp. 5732–5746, 2020.

[12] J. Yao and J. Xu, "Joint 3D maneuver and power adaptation for secure UAV communication with CoMP reception," *IEEE Trans. Wirel. Commun.*, vol. 19, no. 10, pp. 6992–7006, 2020.

[13] M. T. Mamaghani and Y. Hong, "Joint trajectory and power allocation design for secure artificial noise aided UAV communications," *IEEE Trans. Veh. Technol.*, vol. 70, no. 3, pp. 2850–2855, 2021.

[14] Y. Gao, H. Tang, B. Li, and X. Yuan, "Energy minimization for robust secure transmission in UAV networks with multiple colluding eavesdroppers," *IEEE Commun. Lett.*, vol. 25, no. 7, pp. 2353–2357, 2021.

[15] C. Yan, L. Fu, J. Zhang, and J. Wang, "A comprehensive survey on UAV communication channel modeling," *IEEE Access*, vol. 7, pp. 107 769–107 792, 2019.

[16] S. Goel and R. Negi, "Guaranteeing secrecy using artificial noise," *IEEE Trans. Wirel. Commun.*, vol. 7, no. 6, pp. 2180–2189, 2008.

[17] K. Xu, M.-M. Zhao, Y. Cai, and L. Hanzo, "Low-complexity joint power allocation and trajectory design for UAV-enabled secure communications with power splitting," *IEEE Trans. Commun.*, vol. 69, no. 3, pp. 1896–1911, 2021.

[18] M. Cui, G. Zhang, Q. Wu, and D. W. K. Ng, "Robust trajectory and transmit power design for secure UAV communications," *IEEE Trans. Veh. Technol.*, vol. 67, no. 9, pp. 9042–9046, 2018.

[19] H. Lee, S. Eom, J. Park, and I. Lee, "UAV-aided secure communications with cooperative jamming," *IEEE Trans. Veh. Technol.*, vol. 67, no. 10, pp. 9385–9392, 2018.

[20] S. Boyd and L. Vandenberghe, *Convex Optimization*. Cambridge Univ. Press, 2004.

[21] Z. Sheng, H. D. Tuan, A. A. Nasir, T. Q. Duong, and H. V. Poor, "Power allocation for energy efficiency and secrecy of wireless interference networks," *IEEE Trans. Wirel. Commun.*, vol. 17, no. 6, pp. 3737–3751, 2018.

[22] X. Zhou, Q. Wu, S. Yan, F. Shu, and J. Li, "UAV-enabled secure communications: Joint trajectory and transmit power optimization," *IEEE Trans. Veh. Technol.*, vol. 68, no. 4, 4069–4073, 2019.

[23] Q. Wu, Y. Zeng, and R. Zhang, "Joint trajectory and communication design for multi-UAV enabled wireless networks," *IEEE Trans. Wirel. Commun.*, vol. 17, no. 3, pp. 2109–2121, 2018.

[24] M. Grant and S. Boyd, "CVX: Matlab software for disciplined convex programming, version 2.1," http://cvxr.com/cvx, Mar. 2014.